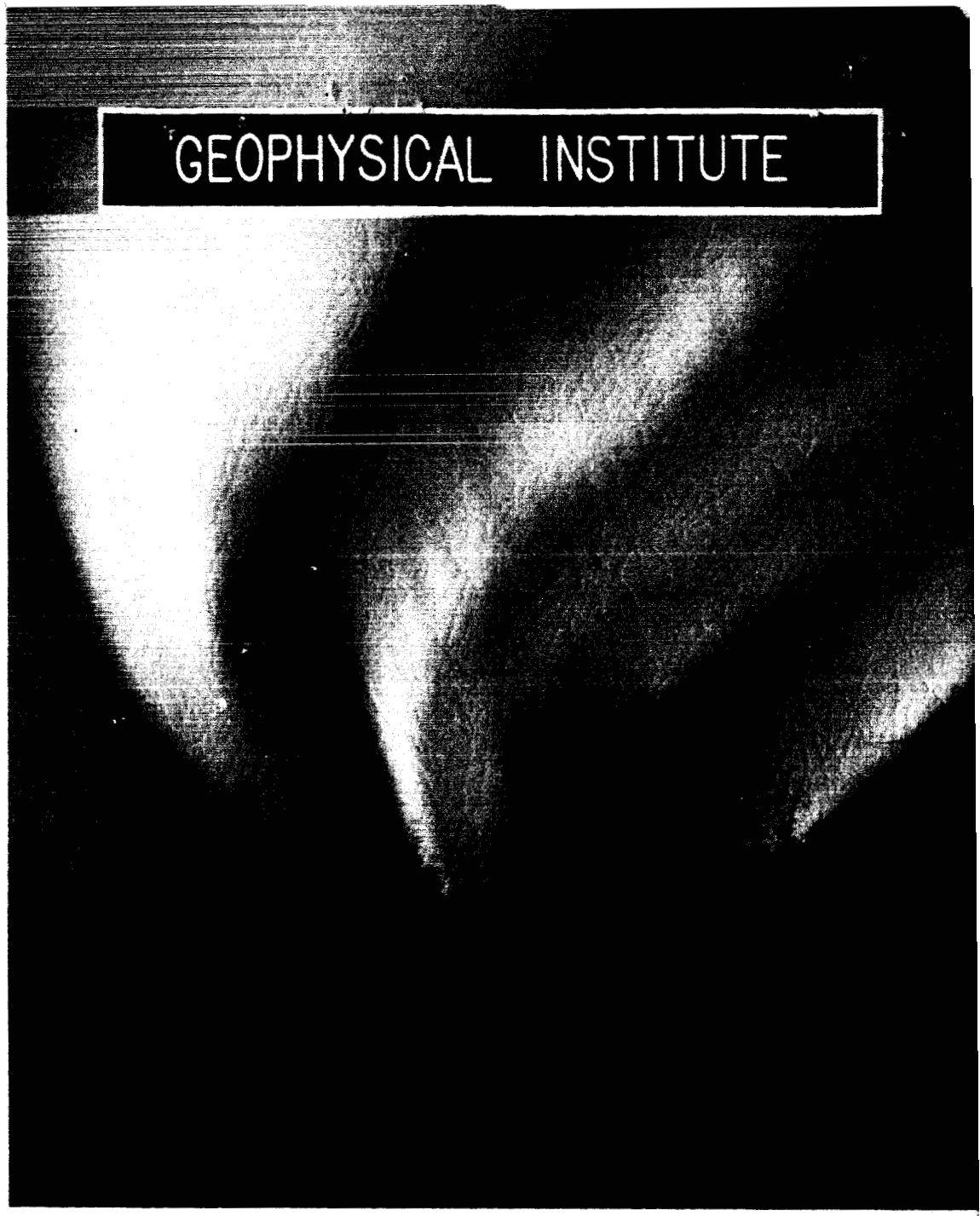

UNIVERSITY
OF ALASKA

COLLEGE
ALASKA

UAG-R136

ELECTRON CONTENT VARIATIONS IN THE AURORAL IONOSPHERE DETERMINED FROM SATELLITE RADIO OBSERVATIONS

by

Jerry L. Hook

Contract No. NAS5-1413
Contract No. Nonr 3010(04)
Scientific Report No. 2

MAY 1963

NATIONAL AERONAUTICS AND SPACE ADMINISTRATION

GEOPHYSICAL INSTITUTE

of the

UNIVERSITY OF ALASKA

ELECTRON CONTENT VARIATIONS IN THE AURORAL IONOSPHERE DETERMINED FROM SATELLITE RADIO OBSERVATIONS

by

Jerry L. Hook

Scientific Report No. 2

Contract No. NAS5-1413

Aberrations of Radio Signals Traversing the Auroral Ionosphere

Contract Nonr-3010(04)

Program of Optical and Radio Measurements within the Auroral Zone in Conjunction with Simultaneous Satellite Measurements

Prepared for

NATIONAL AERONAUTICS AND SPACE ADMINISTRATION
GODDARD SPACE FLIGHT CENTER

DEFENSE ATOMIC SUPPORT AGENCY
OFFICE OF NAVAL RESEARCH
DEPARTMENT OF THE NAVY

Principal Investigators:

Leif Owren
A. E. Belon

Approved by:

C. T. Elvey
Director

ABSTRACT

The Geophysical Institute of the University of Alaska and the Lockheed Missiles and Space Company conducted a joint experiment to study the relationship between (1) spatial distribution of ionization using 20 and 40 mc/s transmissions from a satellite, (2) the location and luminosity profiles of auroras as measured from ground stations in Alaska, and (3) the flux and energy spectrum of particles penetrating to auroral height as measured by satellite instruments. The experiment was carried out in March, 1962 using a polar orbiting satellite which made twelve passes over Alaska during its operational lifetime.

The emphasis of this work is on the determination by radio techniques of the variation of electron content in the ionosphere connected with incident particle fluxes. Methods of determining the electron content from differential Doppler measurements are discussed in detail. The experimental results show that increases in electron content are morphologically correlated with regions of auroral luminosity and incident particle fluxes. The results of the experiment also point out the value of conducting coordinated experiments in the study of auroral phenomena.

ACKNOWLEDGEMENTS

I would like to express my appreciation to Dr. Leif Owren, who was project supervisor for this work and chairman of my advisory committee, and to the other members of my advisory committee, Dr. R. E. Carr and Dr. J. G. Tryon. The author is also grateful to Mr. Albert Belon and Mr. Gerald Romick of the Geophysical Institute staff for many informative discussions.

Acknowledgement is given to Mr. Wilbur Starner for his assistance in carrying out the experiment and to Miss Florence Huang for her assistance in programing the computer and processing of the data. Credit is due to Mr. Dan Wilder for preparing the figures and to Mrs. Zola Wheeler for typing this work in its final form.

This research was supported in part by the Defense Atomic Support Agency, Office of Naval Research under Contract Nonr 3010(04) and by the National Aeronautics and Space Administration under Contract NAS5-1413.

LIST OF ILLUSTRATIONS

CHAPTER I

INTRODUCTION

Radio waves transmitted from artificial earth satellites have been used recently to determine the density and distribution of free electrons in the ionosphere. The integrated electron density along the path of propagation of a radio wave may be determined from the Faraday rotation of the plane of polarization and from the Doppler shift of the received signal. The Faraday effect was first applied using moon radar techniques [Browne, Evans, and Hargreaves, 1956]. Using satellites, Garriott (1960), Little and Lawrence (1960), and Yeh and Swenson (1961) obtained the electron content in a column of unit cross sectional area. The Doppler method was first used with radio transmissions from rockets [Seddon, 1953; Nisbet and Bowhill, 1960] to obtain electron density profiles. The application of the Doppler methods to satellite transmissions have been made by Weeks, (1958), Hibberd and Thomas (1959), Ross (1960), Garriott and Nichol (1961), and de Mendonça (1962) to obtain the electron content.

The information we can obtain is limited to the region lying below the satellite and essentially along the path of propagation. The ray path of the radio wave will approximately sweep out a plane defined by the satellite's trajectory and the receiving station. As a result of this sweeping ray path, it is possible to determine, to some extent as least, the spatial distribution of ionization. Satellites are particularly

advantageous in studying the ionosphere since the velocity of the satellite is so great that drift and random changes in irregularities in electron density can usually be neglected.

The analysis presented here contains part of the results of a joint experiment conducted by the Geophysical Institute and the Lockheed Missiles and Space Co. The main objectives of the experiment are to study the relationship between (1) the flux and energy spectrum of electrons penetrating to auroral heights as measured by satellite instruments, (2) the density and distribution of ionization using 20 and 40 mc/s radio transmissions from a satellite, and (3) the location and luminosity profiles of auroras as measured from a network of ground stations located in Alaska.

In this analysis we obtain the integrated electron density by the Doppler method. The variations in the electron content are then compared with simultaneous measurements of particle fluxes and auroral luminosity. A detailed discussion of the differential Doppler method is given and a general discussion of the Faraday method is presented.

CHAPTER II

DIFFERENTIAL DOPPLER METHOD

A. Doppler Shift

If an antenna which emits electromagnetic waves is moving relative to an observer, then the frequency observed may be different than the emitted frequency. This frequency change is called the Doppler shift and it is given by the relation

$$f_s - f_o = f_s \, (\vec{v}.\vec{r})/c \, , \tag{1}$$

where f_o is the observed and f_s is the emitted frequency. The component of velocity along a straight line from the source to the observer is $\vec{v}.\vec{r}$, where $\vec{v}$ is the velocity of the source, $\vec{r}$ is a unit vector toward the observer, and c is the velocity of propagation in free space. Equation (1) implies that the electromagnetic waves from the source to the observer move through free space.

If the medium is not free space, but a medium whose index of refraction is different from unity, this equation (1) as it stands does not hold. In an ionized medium such as the ionosphere, the index of refraction is not unity, hence the ray path of the electromagnetic wave does not necessarily follow a straight line. At some instant of time, radio waves emitted from the satellite will describe a set of isophase surfaces which will intersect the ray path to the satellite at right angles. For an inhomogenous isotropic medium, the wave is

retarded and subsequently the ray path is "bent" as shown in Figure 1.

B. Phase Path

The basic assumption used in this analysis is Fermat's principle stating that the actual ray path between two points is the shortest time path of propagation, or

$$\delta \int_{s_1}^{s_2} n\,ds = \delta \int_{P_1}^{P_2} c\,dt = 0, \tag{2}$$

where n is the refractive index of the medium. The above equation shows that the time of travel of a wave-front from s_1 to s_2 corresponding to the points P_1 and P_2 along a ray path is stationary with respect to small variations of the path. The total time for a ray to traverse the medium from the observer to the satellite then becomes

$$t = \int_{s_1}^{s_2} \frac{1}{v}\,ds = \frac{1}{c}\int_{s_1}^{s_2} n\,ds. \tag{3}$$

The phase path is defined as

$$P = ct = \int_{s_1}^{s_2} n\,ds. \tag{4}$$

The above expression is not exact for radio waves propagated in an ionized medium. The approximation for the phase path P is valid when refraction varies slowly along the path of

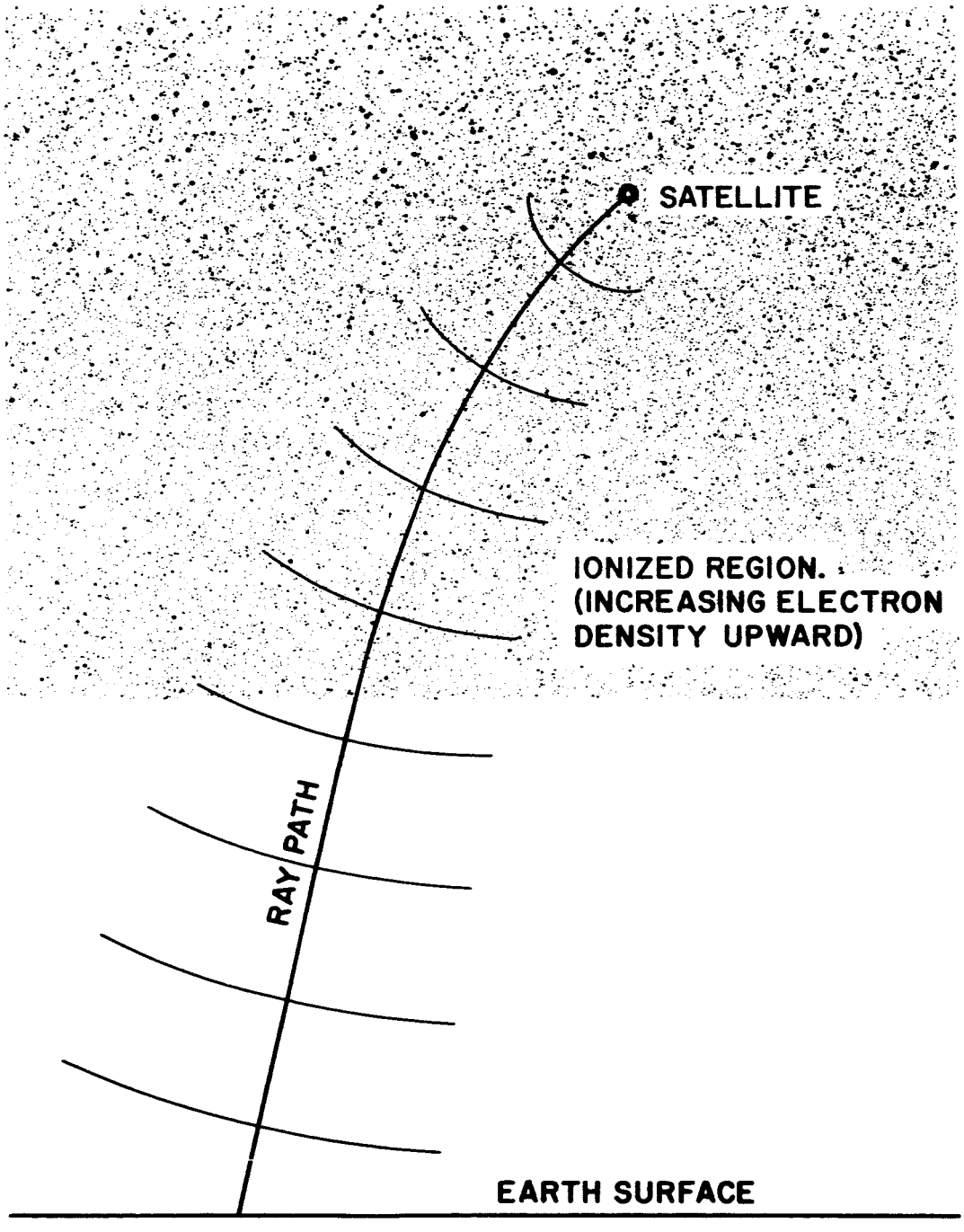

Fig. 1. The bending of the ray path of a radio wave in an ionized medium. The isophase surfaces are shown perpendicular to the ray path.

propagation.

The difference between the phase path P, and a straight line path, R, which is called the phase path defect, (Garriott and Bracewell, 1960), is given by

$$P-R = \Delta P = \int_{o}^{s} (1-n)ds. \tag{5}$$

In the above expression, the refractive index for a given path length determines the magnitude of the phase path defect. In the following section, the refraction of radio waves will be discussed, but the discussion will be limited to those aspects which are relevant to H.F. radio waves in the ionosphere.

C. Refraction in an Ionized Medium

When an electromagnetic wave propagates in an ionized medium, such as the ionosphere, the alternating electric field causes the charged particles in the medium to oscillate. If no binding and frictional forces are present (free particles and lossless medium) and the influence of the magnetic field is neglected, the motion of a charged particle, whose charges and mass are e and m respectively is given by

$$m \frac{d^2 \vec{q}}{dt^2} = e\vec{E}. \tag{6}$$

The vector $\vec{q}$ is the position coordinate of the charge and $\vec{E}$ is the electric field of the wave. For the case of periodic oscillations,

$$\vec{E} = \vec{E}_o e^{i\omega t} \tag{7}$$

and

$$\vec{q} = \vec{q}_o e^{i(\omega t + \psi)} . \tag{8}$$

It follows from equations (6), (7), and (8) that

$$-m\omega^2 \vec{q}_o e^{i\psi} = e\vec{E}_o . \tag{9}$$

In the equation above, the term at the right of the equal sign is positive and real, its phase, therefore, must be $\psi + \pi$ and hence the amplitude of the oscillation of the charge becomes

$$\vec{q}_o = \frac{e}{m\omega^2} \vec{E}_o . \tag{10}$$

From equation (10), it can be seen that electrons will oscillate with considerably greater amplitude than protons or molecular ions, since the mass of an electron is relatively much smaller. It is the free electrons in the ionized medium which mostly affect the propagation of radio waves in the ionosphere.

To quantitatively evaluate the influence of the oscillating electrons on the electromagnetic wave, we start with Maxwell's equations (in MKS Units)

$$\frac{d\vec{B}}{dt} = - \text{curl } \vec{E} \tag{11}$$

$$\vec{B} = n_o \vec{H} \tag{12}$$

$$\frac{d\vec{D}}{dt} + \vec{J} = \text{curl } \vec{H} \tag{13}$$

$$\vec{D} = \epsilon_o \vec{E} \ . \tag{14}$$

In equation (13), the current density is given by

$$\vec{J} = eN\vec{v},$$

where N is the number of charged particles and $\vec{v}$ is their mean velocity. Upon combining the curl of equation (11) with $n_o \frac{d}{dt}$ of equations (13) and (14), the wave equation is obtained.

$$\epsilon_o n_o \frac{d^2\vec{E}}{dt^2} + n_o eN\frac{d\vec{v}}{dt} = - \text{curl curl } \vec{E} \tag{15}$$

$$= \Delta\vec{E} - \text{grad div } \vec{E}$$

$$= \Delta\vec{E}$$

From equation (6)

$$\frac{d\vec{v}}{dt} = \frac{e\vec{E}}{m} \tag{16}$$

and upon substituting this into equation (15)

$$\epsilon_o n_o \frac{d^2\vec{E}}{dt^2} + n_o N \frac{e^2}{m}\vec{E} = \Delta\vec{E} . \tag{17}$$

For simplicity, we assume cartesian coordinates and a plane wave which propagates in the z-direction. The electric field of this plane wave is given by

$$E_x = E_o e^{i\omega(t - \frac{z}{v})}, \tag{18}$$

where v is the phase velocity. The phase velocity in terms of the index of refraction is defined as

$$n = \frac{c}{v} \tag{19}$$

hence,

$$E_x = E_o e^{i\omega(t - \frac{nz}{c})} . \tag{20}$$

When equation (20) is substituted into (17), we obtain

$$-\omega^2 \epsilon_o n_o + n_o N \frac{e^2}{m} = -\frac{\omega^2}{c^2} n^2.$$

Since $\epsilon_o n_o = \frac{1}{c^2}$ in absolute mks units, the index of refraction for the dispersive medium becomes

$$n^2 = 1 - \frac{e^2 N}{\epsilon_o m \omega^2}. \tag{21}$$

The above equation shows that the refraction effect due to electrons is much greater than it is for protons or moleculor ions and upon summing over all charges the electrons are predominant in determining the index of refraction. For the refraction of radio waves in the ionosphere, it is necessary to consider only the electron density, N_e.

For a medium of a given electron density, the frequency at which the index of refraction vanishes is called the critical frequency or plasma frequency of the medium. The lowest satellite frequency which will be considered in this analysis is 20 mc/s, which is usually somewhat greater than the critical frequency of the ionosphere. An average high value of the critical frequency is approximately 10 mc/s.

The effect of an external magnetic field has been neglected in the above discussion. In the ionosphere, the

earth's magnetic field influences the motion of electrons. The refractive index is then non-isotropic, and the general solution for the index of refraction for an arbitrary field direction becomes quite complicated. To simplify the problem, we can for the moment consider two cases, longitudinal and tranverse propagation. In the first case, the wave normal is parallel to the direction of the magnetic field and in the latter the wave normal is perpendicular to the field direction.

We first consider the case of longitudinal propagation of a plane wave in the z-direction. The motion of charged particles as given by equation (6) can be modified to account for an external magnetic field, i.e.

$$m \frac{d\vec{v}}{dt} = e\vec{E} + e(\vec{v}x\vec{B}) . \tag{22}$$

The motion of a charge is in the x-y plane and is given by

$$\left.\begin{aligned} x &= x_o\, e^{i(\omega t + \psi_1)} \\ y &= y_o\, e^{i(\omega t + \psi_2)} \end{aligned}\right\} . \tag{23}$$

A linearily polarized wave propagating parallel to the z-axis at some fixed point has an electric field

$$E_x = E_o\, e^{i\omega t} . \tag{24}$$

For this case, the wave equations are

$$-\omega^2 x_o e^{i\psi_1} = \frac{e}{m} E_o + i\omega \frac{e}{m} B y_o e^{i\psi_2} \tag{25}$$

$$-\omega^2 y_o e^{i\psi_2} = -i\omega \frac{e}{m} B x_o e^{i\psi_1}. \tag{26}$$

The quantity $\frac{e}{m}B$ is called the gyrofrequency and it is the frequency of the circular motion an electron undergoes as a result of the external field, the geomagnetic field in this case. As long as the frequency of the electromagnetic wave is greater than the gyrofrequency, the amplitude of the wave will be little affected by the external magnetic field.

Letting $\omega_H = \frac{e}{m}B$ and solving equations (25) and (26) for y_o and x_o, we have

$$y_o = i\frac{\omega_H}{\omega} x_o e^{i(\psi_1 - \psi_2)} \tag{27}$$

$$x_o = -\frac{e}{m\omega^2} E_o e^{i\psi_1} - i\frac{\omega_H}{\omega} y_o e^{i(\psi_2 - \psi_1)}. \tag{28}$$

The quantities x_o and y_o are real, and therefore, the right hand side of equations (27) and (28) must be real. This condition is satisfied by setting

$$\psi_1 - \psi_2 = \frac{\pi}{2}, \quad \psi_1 = \pi, \text{ and } \psi_2 = \frac{\pi}{2}.$$

From equation (23), the motion of the charges becomes

$$x = - x_o e^{i\omega t}$$

$$y = - i\frac{\omega_H}{\omega} x_o e^{i\omega t} . \qquad (29)$$

The two equations above show that electrons move in elliptic orbits. Of interest here is the case in which the wave frequency is considerably greater than the gyrofrequency, that is, $\frac{\omega}{2\pi} \gtrsim 20$ mc/s and $\frac{\omega_H}{2\pi} \approx 1.0$ mc/s. The major axis of the ellipse is, therefore, considerably greater than the minor axis and as the wave frequency is increased, the electron motion approaches a linear oscillation. An electromagnetic wave of a given polarization acts on the electrons and because of elliptic orbits of the electrons, the secondary waves are polarized differently than the primary waves. In the medium, the polarization of the primary wave is continuously altered and if the primary wave was originally linearly polarized, the resulting wave will be elliptically polarized. For an electromagnetic wave incident parallel to the magnetic field, two wave modes with opposite polarizations will be propagated. The two corresponding indices of refraction for the longitudinal mode of propagation are (Rawer, 1952), if $\omega_H < \omega$,

$$(n_{o,x})^2 = 1 - \frac{e^2 N}{\epsilon_o m\omega(\omega \pm \omega_H)} = 1 - \frac{f_o^2}{f(f \pm f_H)} , \qquad (30)$$

Where $f_o = (\frac{e^2N}{\epsilon_o m})^{1/2}$ is the plasma frequency of the medium. The subscript "0" refers to the so called ordinary component (upper sign) and the "X" refers to the extraordinary component (lower sign) of the two oppositely rotating polarizations.

Only the longitudinal mode of propagation has been considered in the above discussion. When the direction of the magnetic field is perpendicular to the wave normal, we have the tranverse case. If the polarization of the incident wave is parallel to the direction of the magnetic field, the field will have no effect on the motion of the electrons. The index of refraction for this case is

$$n^2 = 1 - \frac{f_o}{f^2}, \tag{31}$$

where f_o is the plasma frequency and f the wave frequency. The above relation is equivalent to the case where the magnetic field has been omitted as in equation (21). On the other hand, if the incident wave is polarized perpendicular to the direction of the magnetic field, the electrons will describe ellipses in a plane perpendicular to the magnetic field. The index of refraction for perpendicular polarization is (Rawer, 1952)

$$n^2 = 1 - \frac{f_o^2(f^2-f_o^2)}{f^2(f^2-f_o^2-f_H^2)} . \tag{32}$$

The linear polarization normal to the magnetic field is preserved.

In practice the wave normal will be oblique to the direction of the magnetic field and in this case the equation for the index of refraction is quite complicated. The collision free form of the Appleton-Hartree formula for the index of refraction for an arbitrary angle, θ, between the magnetic field vector and the wave normal is (Rawer, 1952)

$$n^2 = 1 - \frac{f_o^2}{f^2 - \frac{f_H^2 f^2}{2(f^2 - f_o^2)} \sin\theta \pm \left\{ f_H^2 f^2 \cos^2\theta + \left[\frac{f_H^2 f^2}{2(f^2 f_o^2)} \sin^2\theta \right]^2 \right\}^{1/2}} \quad (33)$$

Booker (1935) has shown that in practice either the quasi-longitudinal (QL) or quasi-transverse (QT) approximation can usually be used. The applicability of one or the other approximations depends upon the condition

$$\frac{1}{2} \frac{\sin^2\theta}{\cos\theta} f_H < \frac{1}{3} \frac{f^2 - f_o^2}{f} \text{(QL case)} \quad \text{or} \quad \frac{1}{2} \frac{\sin^2\theta}{\cos\theta} f_H > 3 \frac{f^2 - f_o^2}{f} \text{(QT case)}.$$

The factor 3 and $\frac{1}{3}$ in the above inequalities are arbitrarily chosen to give reasonably accurate numerical values for ionospheric calculations (Ratcliffe, 1959). For the wave frequencies of interest here ($f \geqslant 20$ mc/s), the QL approximation will hold for most cases. For example, let f=20 mc/s, f_o=10 mc/s, and f_H=1.5 mc/s. The QL approximation in this case holds for $0 < |\theta| < 84°$. On the other hand the QT approximation holds only for $89° < |\theta| < 90°$.

D. Differential Doppler Shift

In section A the phase path is given by equation (4) and it is assumed that the refractive index varies slowly along the path of propagation. Due to the motion of a satellite, the phase path is continually changing as the time varies. The rate of change of the path can, therefore, be expressed as a time derivative of P. In terms of a Doppler shift,

$$f_s - f_o = \frac{\dot{P}}{\lambda}, \tag{34}$$

where $\dot{P}$ is the time derivative of the phase path and λ is the wave length of the observed frequency f_o. The frequency radiated by the satellite is f_s. The above equation would be equivalent to the Doppler shift given by equation (1) if the radio wave were propagating through free space. The Doppler shift depends not only on the frequency of the radio wave, but also on the phase path, as shown by equation (34). The difference between the Doppler shift observed when a radio wave passes through an ionized medium and the Doppler shift that would have been observed in absence of the ionized medium is called the differential Doppler shift. The differential Doppler shift is quite small, usually much smaller than the Doppler shift, $f_s - f_o$. It is, therefore, necessary to measure the observed frequency very accurately. The frequency of the source (the frequency radiated by the satellite transmitter) is not absolutely stable and it may fluctuate in frequency as much

or more than the differential Doppler effect. A simple method has been devised to overcome this difficulty and this is done by radiating two phase coherent or harmonically related frequencies (Seddon, 1953). Since the index of refraction depends upon the wave frequency, each harmonically related frequency will have a different index of refraction in the ionized medium. Upon receiving these two frequencies at the observer's location, one of the frequencies may be multiplied or divided by the ratio of the harmonic frequencies and then the rate of change of phase between these frequencies can be recorded. The difference in frequency will depend for the most part on the index of refraction refraction of the lower frequency.

The phase path defect resulting from the different indices of refraction for two harmonically related frequencies is the difference in the phase path. Thus from equation (4)

$$\Delta P = P_1 - P_2 = \int_0^s (n_1 - n_2)\,ds, \tag{35}$$

where P_1 and P_2 are the phase paths for the higher and lower frequencies respectively. It will be assumed that the index of refraction is nearly unity. Equation (21) then can be to a good approximation given by

$$n = \left[1 - \frac{e^2 N}{\epsilon_o m \omega^2}\right]^{1/2} \cong 1 - \frac{e^2 N}{2\epsilon_o m \omega^2} \tag{36}$$

In rationalized mks units, with N denoting the electron density per cubic meter and the frequency ,f , expressed in cycles per second, this gives

$$n \cong 1 - \frac{40.3N}{f^2} = 1 - \frac{K_1 N}{f^2}. \tag{37}$$

Upon substituting the index of refraction given by equation (37) into equation (35) and letting rf be the harmonic frequency, we obtain

$$\Delta P = \frac{K_1}{f^2} \left(\frac{r^2-1}{r^2}\right) \int_0^S n\,ds. \tag{38}$$

The straight line path from the observer to the satellite can be represented by

$$R = \int_0^S ds. \tag{39}$$

In terms of the zenith angle χ and height h_s of the satellite,

$$ds = \sec \chi \; dh \tag{40}$$

and

$$R = h_s \sec \chi \; . \tag{41}$$

Since χ varies slowly along the ray path, equation (38) can be expressed approximately as

$$\Delta P \cong \frac{K_1}{f^2}\left(\frac{r^2-1}{r^2}\right)\sec\chi \int_o^{h_s} N dh \qquad (42)$$

The integrated term is the equivalent vertical electron content, that is the total number of electrons in a column of unit base which extends from the ground to the height of the satellite. It should be emphasized here that the electron content is the result of integrating the electron density along the path of propagation. To obtain an equivalent vertical electron content, the obliguity of the phase path is taken into account by the sec χ factor.

By the two frequency method, the beat frequency observed or the differential Doppler frequency is the time rate of change of $\frac{\Delta P}{\lambda}$. The quantity $\frac{\dot{\Delta P}}{\lambda}\frac{r^2-1}{r^2}$ (where the dot is the derivative with respect to time) is called the Doppler shift offset (Garriott and Bracewell, 1960). Differentiating equation (42) with respect to time, and dividing by

$$\frac{\dot{\Delta P}}{\lambda} \cong \frac{K_1}{\lambda f^2}\left(\frac{r^2-1}{r^2}\right)\left[\int_o^{h_s} N dh \frac{d}{dt}\sec\chi + \sec\chi \frac{d}{dt}\int_o^{h_s} N dh\right] . \qquad (43)$$

Let

$$I = \int N dh \text{ and } \left[\frac{K_1}{\lambda f^2}\left(\frac{r^2-1}{r^2}\right)\right] = C_1 ,$$

then (43) can be written

$$\dot{I} + \left[\cos\chi \frac{d}{dt}\sec\chi\right] I = \frac{\cos\chi}{C_1} \frac{\Delta\dot{P}}{\lambda} . \qquad (44)$$

Equation (44) is a first-order and linear differential equation.

The functions of χ are known functions of time when the orbit of the satellite is known. To calculate I(t) we need one initial condition, that is the value of I at some arbitrary time.

CHAPTER III

FARADAY ROTATION

The presence of the earth's magnetic field in the ionosphere causes the plane of polarization of a radio wave to rotate as the wave propagates through the ionosphere. This rotation is known as the Faraday effect. A plane polarized wave propagating parallel to the magnetic field upon entering the ionosphere is split into two circularly polarized modes which have opposite senses of rotation. Because each mode has a slightly different index of refraction, the phase between the two modes is continually changing. Upon combining the two modes at any point along the path, the resulting polarization will be linear, but it will have rotated in a plane perpendicular to the direction of propagation. The angle Ω which the polarization has rotated is related to the difference in phase path of the two modes by

$$\Omega = \frac{\pi f}{c}(P_o - P_x), \tag{45}$$

where P_o and P_x are the phase paths of the ordinary and extraordinary modes. Equation (30) gives the index of refraction for the two modes. If we assume the two modes propagate along the same path, then by substituting equation (30) into (45) and integrating along the phase path, we obtain

$$\Omega = \frac{e^3 n_o}{16 \pi^3 m^2 \epsilon_o c f^2} \int_o^{h_s} NH \cos\theta \sec\chi \, dh. \tag{46}$$

where Hcos θ is the component of the geomagnetic field along the direction of propagation. The rate of rotation of the plane of polarization can be obtained by differentiating the above equation with respect to time. Since both Hcos θ and sec χ vary slowly with respect to time, equation (46) can be expressed:

$$\Omega(t) \cong \frac{K_2 H\cos\theta \ \sec\chi}{f^2}\int_0^{h_s} Ndh = \Omega_o + \Delta\Omega_i \qquad (47)$$

where $K_2 = \dfrac{e^3 n_o}{16\,\pi^3 m^2 \epsilon_o c} = 4.72(10^{-3}), \left[\text{mks}\right]$. The quantity $\Delta\Omega_i$ can be measured and Ω_o is a constant. If the height of the satellite is not too great, the value of Hcos θ is nearly constant along the phase path. By assuming a model for the geomagnetic field and knowing the position of the satellite, the value of Hcos θ can be calculated as a function of time. If the value of Ω_o can be determined, the electron content as a function of time can thus be obtained from the measurement of Faraday rotation. It can be seen that equation (47) is similar to equation (42) and that both expressions contain the integrated electron content $\int Ndh$.

CHAPTER IV

THE CALCULATION OF ELECTRON CONTENT

In chapter II it was shown that the electron content as a function of time could be calculated by solving the differential equation (44). To calculate the electron content, however, one initial condition is required, namely the value of the electron content for an arbitrary time. Since this initial condition is not known, it is necessary to use other observational data or techniques to establish its value. In the following sections (A) and (B), two methods of obtaining the initial condition will be described. The first method is a least square approximation technique which requires no other observational data, but the calculations require the use of a digital computer. In the second method Faraday rotation information and a model for the earth's magnetic field are required, but the calculations to obtain the electron content are simpler than the least square method.

A. Least Square Method

In this section a least square approximation technique devised by de Mendonça (1962) to calculate the electron content using only differential Doppler information will be described. A further refinement of this least square technique which properly accounts for horizontal gradients in electron density is presented.

The phase path difference, ΔP can be obtained by integrating the differential Doppler measurement, thus

$$\Delta P = \Delta P_o + \lambda \int_{t_1}^{t_2} \left(\frac{\Delta \dot{P}}{\lambda} \right) dt \equiv \Delta P_o + \Delta P_i, \tag{48}$$

where ΔP_o is an unknown initial condition and ΔP_i is understood to be $\sum_{i}^{n} \Delta P_i$. The time integral of the differential Doppler frequency multiplied by the wavelength can be obtained numerically by counting the number of cycles of the differential Doppler measurement from time t_1 to t_2.

From the geometry of the satellite orbit relative to the receiving station, there is a time when the zenith angle of the ray path is a minimum, hence

$$\frac{d}{dt} \left[\cos \chi (t) \right]_{t=t_o} = 0. \tag{49}$$

The electron content given by equation (44) for $t=t_o$ then reduces to

$$\dot{I}(t_o) = \frac{\cos \chi (t_o)}{C_1} \frac{\Delta \dot{P}(t_o)}{\lambda} . \tag{50}$$

The above expression is a first linear approximation for $\dot{I}(t)$, the time rate of change of the electron content of a column having unit base. If the measured value of $\frac{\Delta \dot{P}_i}{\lambda}$ in the

neighborhood of t_o is quite irregular, an average value can be used. Using equation (44) we can obtain a first approximation for the differential Doppler shift,

$$F_1(t) = C_1\left[I(t)\frac{d}{dt}\sec X(t) + \dot{I}_1(t)\sec X(t)\right] \tag{51}$$

$$= \left[\frac{\cos X(t_o)}{\cos X(t)}\left(\frac{\Delta\dot{P}(t_o)}{\lambda}\right) - \frac{(\Delta P_o+\Delta P_i)}{\lambda\cos X(t)}\frac{d}{dt}\cos X(t)\right], \tag{52}$$

where $I(t_o)=I_1(t)$. All of the quantities in this equation are known except ΔP_o. The zenith angle functions can be calculated from the known orbit of the satellite.

We can approximate the value of ΔP_o by a least square method. The usual technique is to sum the squares of the deviations, hence

$$E_1 = \sum_i (F_i - \frac{\Delta\dot{P}_i}{\lambda})^2 . \tag{53}$$

The value of ΔP_o which will minimize the sum is then used to calculate a first approximation of the electron content $I_1(t_i)$ (the subscript i refers to $I_1(t)$ at discrete times (t_i). The minimization of (53) can readily be accomplished with a digital computer. From equations (42) and (48), we have

$$I(t_i) = \frac{(\Delta P_o+\Delta P_i)\cos X}{\lambda C_1} \tag{54}$$

Once $I_1(t_i)$ has been obtained, it can be used to find a second approximation for the electron content by an iterative process.

A best fit polynomial can then be found which will represent the curve defined by $I_1(t_i)$, i.e.

$$I_1(t) = a_1+a_2t+a_3t^2+,- - - -,+ a_nt^n. \tag{55}$$

The curve for $I_1(t_i)$ is usually smooth with no more than two maxima or minima and, therefore, in most cases a third degree polynomial will adequate. The second approximation for $\dot{I}(t)$ is obtained by taking the time derivative of (47), thus

$$\dot{I}_2(t) = a_2+2a_3t+3a_4t^2+,- - - -,+na_nt^{n-1}. \tag{56}$$

The above function is then used to obtain a new function, $F_2(t)$, for the differential Doppler frequency

$$F_2(t) = \left[I(t)\frac{d}{dt}\sec\chi(t)+\dot{I}_2(t)\sec\chi(t)\right] \tag{57}$$

A new value for ΔP_o can be calculated by minimizing

$$E_2 = \Sigma_i \left[(F_2)_i - \frac{\Delta\dot{P}_i}{\lambda}\right]^2. \tag{58}$$

When ΔP_o has been found, $I_2(t_i)$ can be calculated. The process given above may be repeated to find $I_3(t)$, $I_4(t)$, ----, $I_n(t)$, until

$$\left| I_{n-1} - I_n \right| < \epsilon ,$$

where ϵ is an arbitrary value representing the maximum deviation of I(t).

A great many numerical calculations are required to obtain the electron content, I(t), for a single satellite passage. During an average satellite passage, the differential Doppler shift is recorded for approximately three minutes and if I(t) is calculated at one second intervals, then 180 data points are carried in the calculations. The only practical way to do these calculations is to use a digital computer.

B. Combined Doppler-Faraday Method

The electron content is related to both the differential Doppler frequency and the Faraday rotation rate. It is possible to combine these measurements as suggested by Burgess (1961) to calculate the electron content. By this method the constant ΔP_o can be calculated directly and no assumptions about horizontal gradients in the electron density or vertical velocity components of the satellite are required. Methods for calculating the electron content using Faraday and Doppler

information have been devised by Golton (1962) and de Mendonça and Garriott (1962b), and the latters method will be described here.

The Doppler and Faraday effects are independent from one another and, therefore, it is possible to combine equations for ΔP (42) and Ω (47) and obtain

$$\Omega = \frac{K_2 H \cos\theta}{K_1} \Delta P = K_3 H_L \Delta P \quad , \tag{59}$$

where H_L is the magnetic field in the direction of wave normal. For any two arbitrarily chosen times t_1 and t_2,

$$\Omega_{1,2} = K_3 \left[H_{L_1} \Delta P_1 - H_{L_2} \Delta P_2 + H_{L_1} \Delta P_o - H_{L_2} \Delta P_o \right] \tag{60}$$

and solving for ΔP_o, we have

$$\Delta P_o = \left[\frac{\frac{\Delta \Omega_{1,2}}{K_3} + \Delta P_2 H_{L_2} - \Delta P_1 H_{L_1}}{H_{L_1} - H_{L_2}} \right] . \tag{61}$$

All of the quantities on the right side of the above equation can be measured experimentally or calculated. Upon differentiating equation (59) with respect to time, we obtain

$$\Delta P = \frac{\dot{\Omega}}{K_3 \dot{H}_L} - \frac{H_L \Delta \dot{P}i}{\dot{H}_L} \quad , \tag{62}$$

where $\Delta P = \Delta P_o + \Delta Pi$ (equation 48).

The above equation is useful since the time rate of change of Ω and ΔP are usually measured directly.

The value of ΔP_o obtained by the Doppler-Faraday method and by the least square approximation method described have been compared by de Mendonça and Garriott (1962 b). They have found that both methods give similar results, within 5%, for cases where the Faraday rotation rate was not too slow. When the total Faraday rotation is less than 10 radians, they suggest that ΔP_o obtained by the least square approximation is more accurate.

C. Faraday Effect on the Differential Doppler Measurement

In obtaining the electron content from the differential Doppler measurement, the effect of the earth's magnetic field has been neglected. de Mendonça and Garriott (1962c) have shown that the error is small when the magnetic field is neglected in the calculations.

The index of refraction given by equation (30) is slightly different for ordinary and extraordinary mode, since the radio frequencies used for satellite transmissions are usually much greater than the gyrofrequency of the medium.

The phase path for each of the two modes of propagation will not be the same and as a result the Doppler shift for each mode will be different. The Doppler shift measurement will correspond to the mode which is accepted by the antenna. If a linearly polarized antenna is used, such as a dipole, the

antenna will receive both circularly polarized modes. The frequency of the signal that is received by the antenna can be determined in the following way. Let the voltage induced on the receiving antenna by the ordinary and extraordinary waves be

$$E_o = A \sin 2\pi f_o t \tag{63}$$

and

$$E_x = B \sin 2\pi f_x t$$

$$= B \sin 2\pi (f_o + 2f_1) t , \tag{64}$$

where $2f_1 = f_x - f_o$ is the frequency difference between the ordinary and extraordinary waves. This frequency difference is a result of the slightly different Doppler shift of the two wave modes. The total voltage induced on the antenna is

$$E = E_o + E_x = A \sin 2\pi f_o t + B \sin 2\pi (f_o + 2f_1) t . \tag{65}$$

When the ordinary wave predominates, i.e. $A \gg B$, and the differential Doppler shift will correspond to the ordinary wave. In the case $A=B$, both modes will be received equally by the antenna. We have then, letting $A=B=C$

$$E = c\left[\sin 2\pi f_o t + \sin 2\pi (f_o+2f_1)t\right]$$

$$= 2c \sin\left[2\pi (f_o+f_1)t\right] \cos 2\pi f_1 t . \qquad (66)$$

The frequency of the two modes combined at the antenna in this case will be

$$f_o+f_1 = \frac{1}{2}(f_o+f_x)$$

or the mean value of f_o and f_x. The $\cos 2\pi f_1 t$ term will modulate the received signal at a frequency f_1, since f_o and $f_x \gg f_1$. The frequency f_1 is equal to the Faraday fading rate.

radiated linearly polarized waves at the harmonically related frequencies of 20 and 40 mc/s. At the receiving station, linearly polarized, three-element yagi antennas were used on each frequency. The antennas were spaced approximately one wave length apart along a line perpendicular to the subsatellite path.

A phase-lock system was used to "lock" the phase of the received signal to a 455 kc/s reference oscillator. Common oscillators for both the 20 and 40 mc/s receivers were used to retain the phase relationship between the two signals. In order to compare the relative phase of the two signals, the frequency resultant of the first converter of the 20 mc/s system is doubled and then applied to its IF amplifier. The differential Doppler shift is obtained by recording the phase between the 455 kc/s reference oscillator and the IF output of the 20 mc/s receiver. Along with the differential Doppler shift, the 40 mc/s Doppler shift is recorded. The Doppler shift appears as the difference frequency between the tracking oscillator and a stable 40.460 mc/s crystal oscillator.

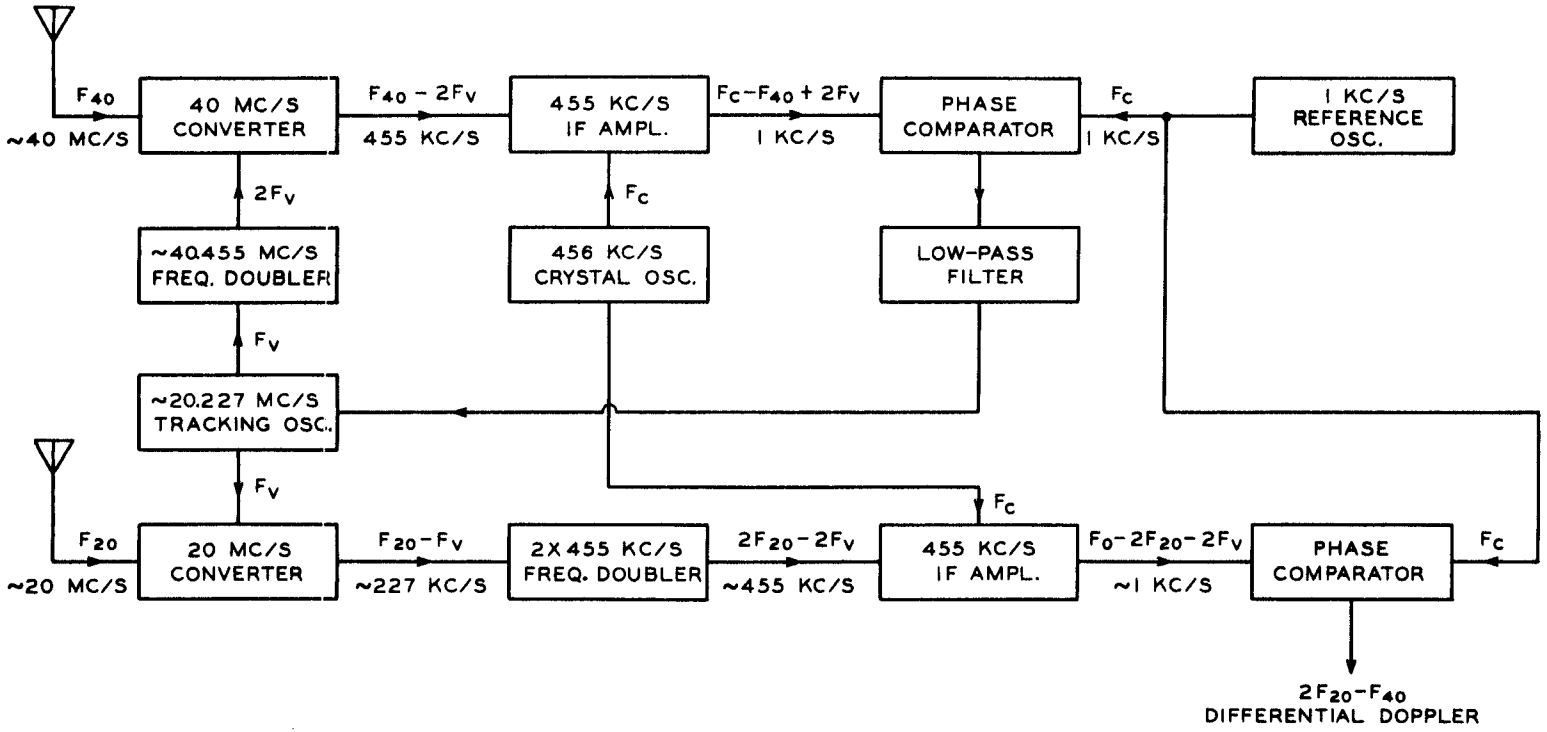

Fig. 2. Block diagram of the experimental equipment used to record the differential Doppler shift.

CHAPTER VI

EXPERIMENTAL RESULTS

Differential Doppler measurements were obtained from four passages of the satellite 1962ϵ over College, Alaska (Geomagnetic latitude 64.65°N, longitude 256.56°E), between March 1 and March 4, 1962. The electron content has been calculated and in this chapter the results of these calculations will be presented and discussed. Besides the differential Doppler measurements recorded, direct measurement of particles fluxes, radio wave diffraction measurements, and optical measurements on auroras were made simultaneously during several of the satellite passages. The relationship between these other measurements and the electron content of the ionosphere will also be discussed.

The satellite was injected into a nearly polar orbit on February 28, 1962. The orbit was inclined approximately 82°. The height of the satellite when it passed over the vicinity of College ranged between 255 and 280 km. For the south to north passages over College, the satellite's motion was nearly parallel to the College geomagnetic meridian. Shown in Figure 3 are the subsatellite paths relative to College for the four passages of the satellite which will be considered in this analysis. The thick portion of the lines representing the subsatellite paths indicate the location of the satellite when differential Doppler data were obtained.

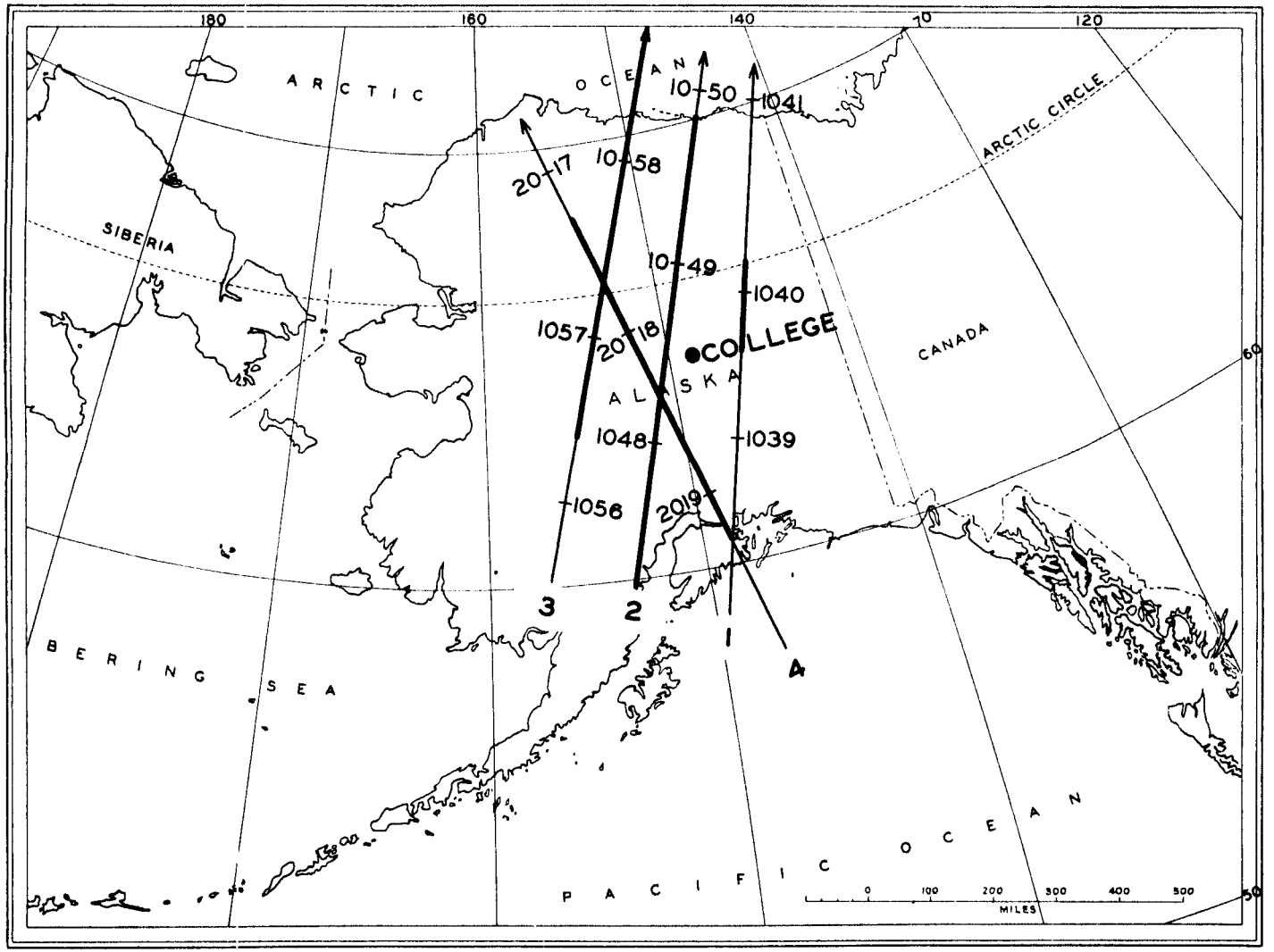

Fig. 3. Map of Alaska showing the subsatellite paths for satellite passages 1,2, 3, and 4. The thick portion of the subsatellite lines indicate the time when differential Doppler data were recorded.

The electron content was calculated using the initial condition, ΔP_o, determined by the least square method discussed on pages 25-27. The first approximation of ΔP_o was used in the calculation of the electron content for the four satellite passages. Higher order approximations of ΔP_o were not calculated because not enough time was available to develop the necessary computer programs to do these calculations. The electron content calculated by using the first approximation of ΔP_o may be in error a few per cent, but the relative variations in the electron content will be quite accurate. In this analysis we are concerned mostly with the relative variations of the electron content.

A plot of electron content I(t) (which will be referred to hereafter as I) as a function of time for satellite passage number 2 of the satellite is shown in Figure 4. The satellite passage numbers are arbitrarily chosen. The plot at the bottom of this Figure shows a distribution of diffracting irregularities in electron density. See the Appendix for a brief discussion of the experimental technique used to determine the height of diffracting irregularities. Also shown in Figure 4 are the times when the total energy detectors on board the satellite registered high particle counts. The two total energy detectors had thresholds of 4 and 33 kev for electrons and they accepted particles with pitch angles up to approximately 43° (Meyerott and Evans, 1962). The particle flux was observed from 1048:33 to 1048:38 UT when telemetry acquisition

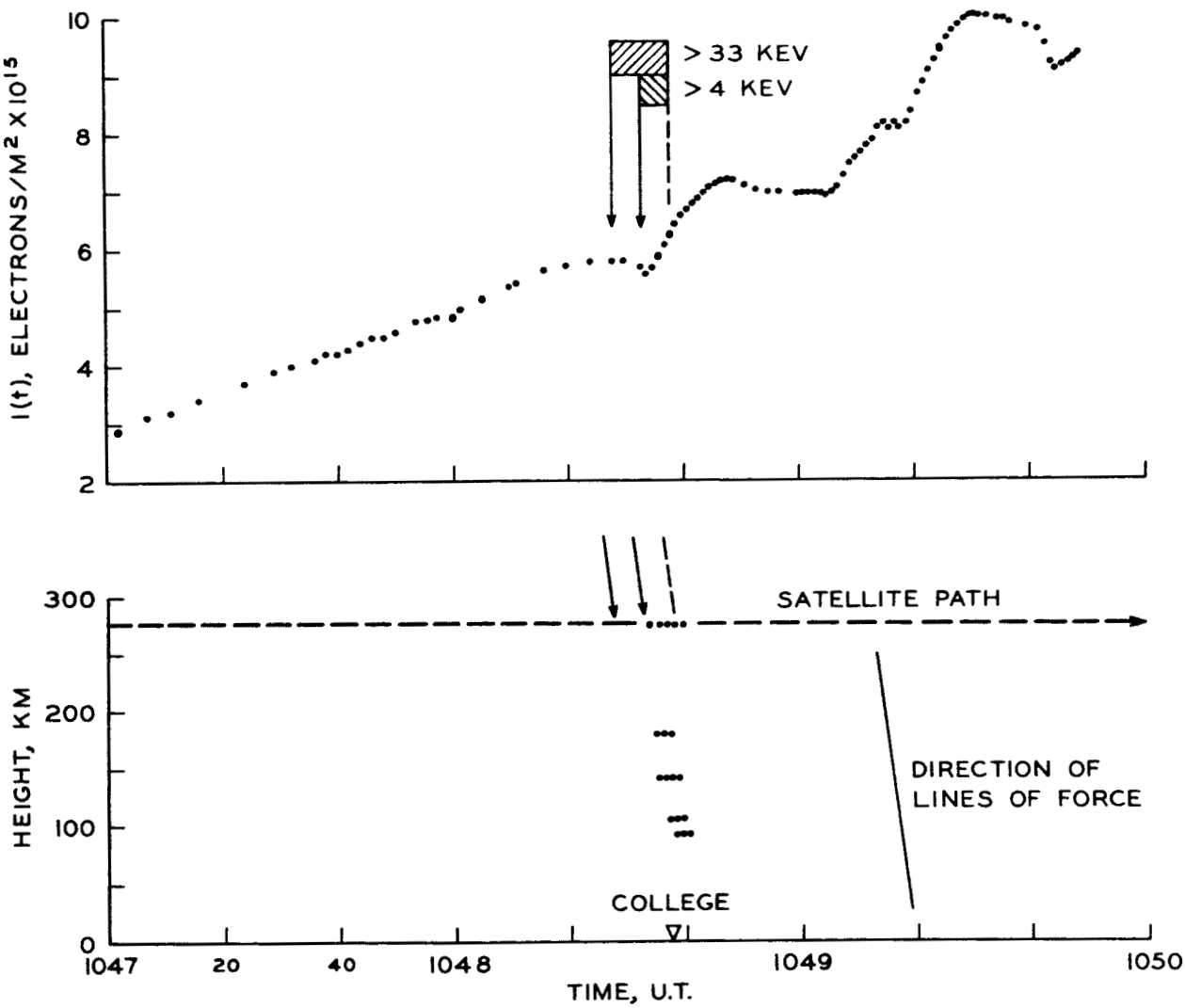

Fig. 4. The electron content as a function of time (top) and the distribution of irregularities in the plane of the magnetic meridian (bottom) for passage number 2. Also shown are the times when energetic particles were defected.

ended. As indicated in Figure 4, the particles were observed when the satellite intersected the lines of force along which irregularities were observed.

The plot of I in Figure 4 is characterized by a relatively smooth but steady increase of I as the satellite proceeded northward. Relatively sharp increases of I are evident after 1048:35 UT. The rapid increase of the quantity I from 1048:35 to 1048:48 UT could be due to ionization produced by the particle flux in the region where irregularities are located. Since particle data acquisition ended at 1048:38 UT, it is not known whether or not the other variations of I are possibly due to ionization by primary particles. Cloudy weather prevailed during this passage of the satellite and, therefore, observation of the aurora was not possible.

In Figure 5, a similar pair of plots for satellite passage number 1 are shown. Phase-lock of the receiving equipment was not achieved until 1039:34 UT and as a result differential Doppler data was not obtained prior to this time.

In the lower plot of Figure 5, a cross-section of an auroral form is shown by the cross-hatched area. The location of the region of auroral luminosity was determined by (Belon and Owren, 1962) using scanning photometers sensitive to 3914, 5577, and 6300 Angstrom emission. High particle counts were registered between 1039:54 and 1039:58 UT by the 4 and 33 kev total energy detectors. As indicated in Figure 5, the particle flux corresponds quite well with the region of auroral

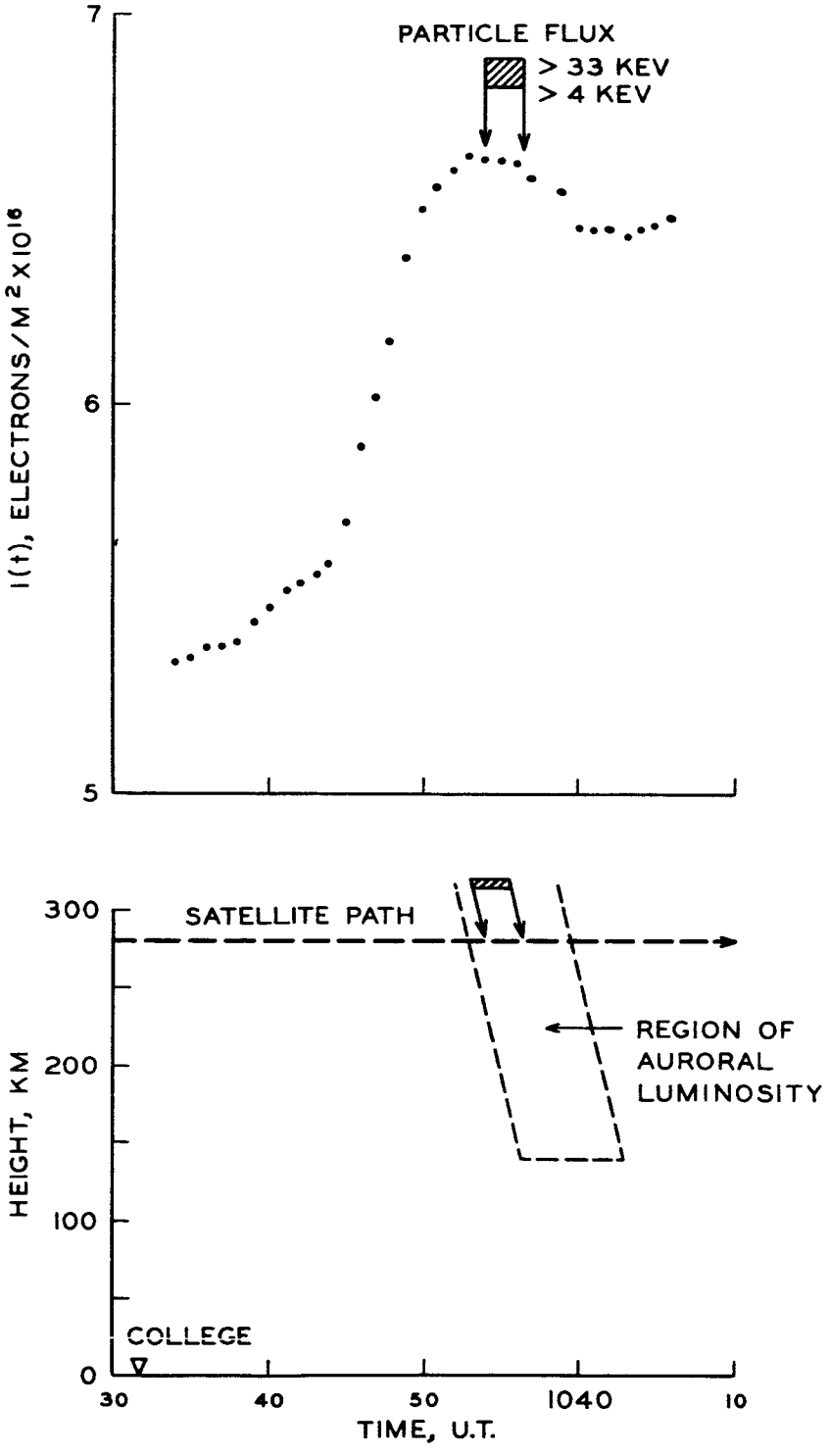

Fig. 5. The electron content as a function of time (top) and the distribution of irregularities in the plane of the magnetic meridian (bottom) for passage number 1. Also shown are the times when energetic particles were defected.

luminosity. As seen in the upper plot, the value of I increases rapidly as the satellite approaches the region of auroral luminosity and reaches a maximum at approximately the time that the satellite penetrates the region of luminosity. Upon entering the auroral form, the value of I remains near its maximum value until the end of the data.

It is possible in this case to make a first order approximation as to where along the path of propagation the region of increased electron density was first encountered. Since amplitude scintillations were weak during this period, the fading rate of the signals due to the Faraday rotation of the plane of polarization was observed. The fading was observed at College and at a receiving station located 9 km north of College, These two stations formed a line which was nearly parallel to the subsatellite path. By the same method whereby the heights of irregularities are determined, it is possible to find the approximate height at which the region of increased electron density was first encountered. At the time when the electron content was rapidly increasing, a corresponding increase in the rate of Faraday fading was observed. A plot of the Faraday fading period from College and Murphy Dome sites, which are approximately 9 km apart, is shown in Figure 6. Between 1039:45 and 1039:49 UT, it appears that the maximum fading rate for the two stations occurs nearly simultaneously. A displacement of the maximum fading rate of 2 sec. would give a calculated height of 100 km. It appears then that the region

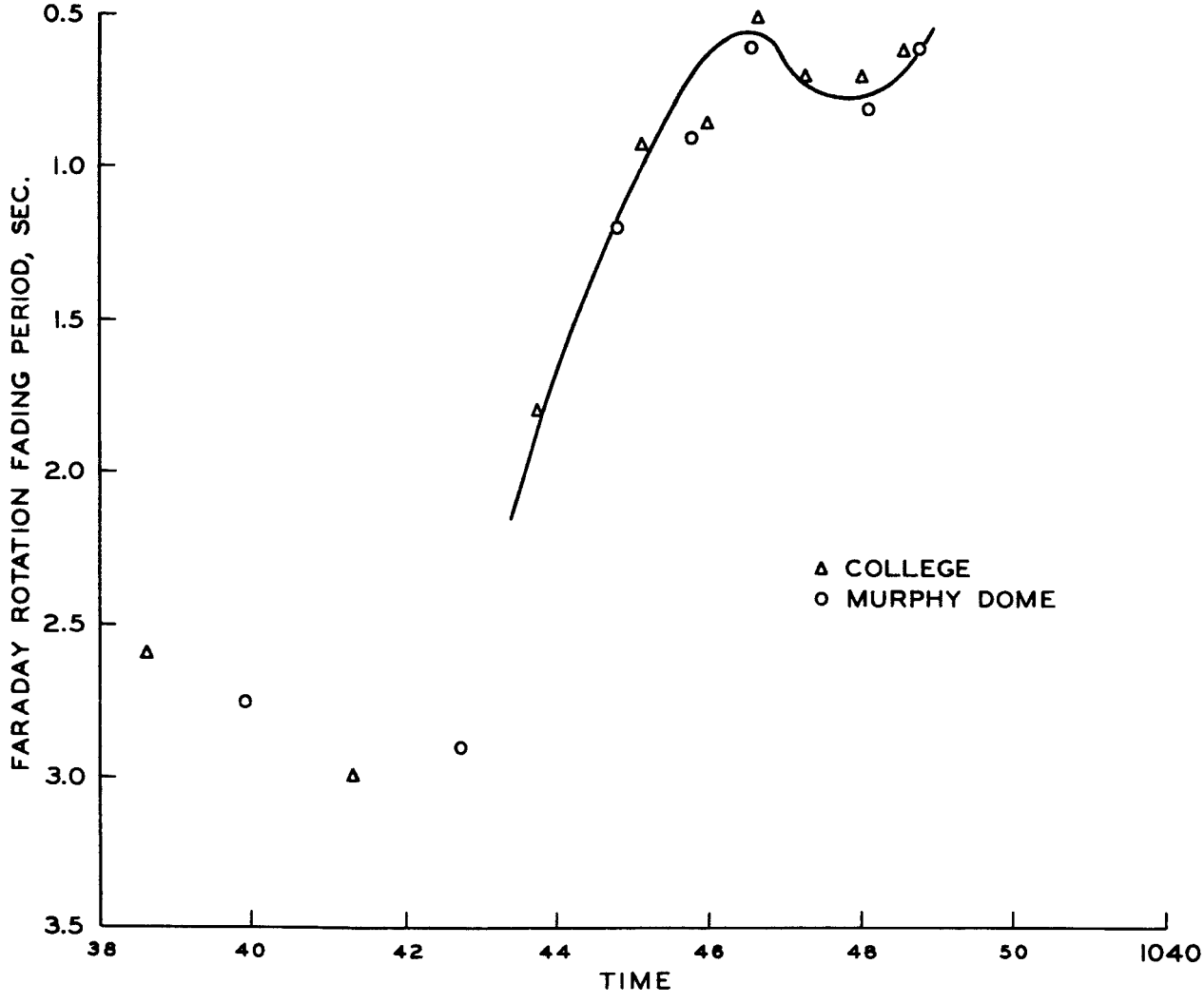

Fig. 6. The Faraday rotation period as a function of time observed at College and Murphy Dome sites.

of increased electron density was first encountered in the vicinity of the satellite as would be expected when the satellite passes through the region of auroral luminosity.

A similar pair of plots of I and the distribution of irregularities for passage number 3 are shown in Figure 7. In the lower plot, a rather extensive vertical distribution of irregularities is indicated. The north-south extent of these irregularities, as indicated by the plot, is in the order of 150 km. There is a broad maximum in the electron content centered about the region where the vertical distribution of irregularities were observed. The particle detector data have not been evaluated for passage number 3 yet, but a preliminary inspection of the data indicated possible high particle counts occurred just prior to 1057:00 UT. Auroras were observed somewhat to the north of College which corresponds approximately to the time when the electron content began to increase at 1058:30 UT.

In the three preceding passages discussed, the satellite passed over College near local midnight. In Figure 8, the plot of electron content and distribution of irregularities are for a daytime passage of the satellite. The trajectory of the satellite in this case was skewed approximately 30° to the College geomagnetic meridian. In the lower plot (Figure 8), an extensive vertical distribution of irregularities is indicated. This distribution of irregularities appears to correspond with the maximum in electron content calculated between 2017:20 and

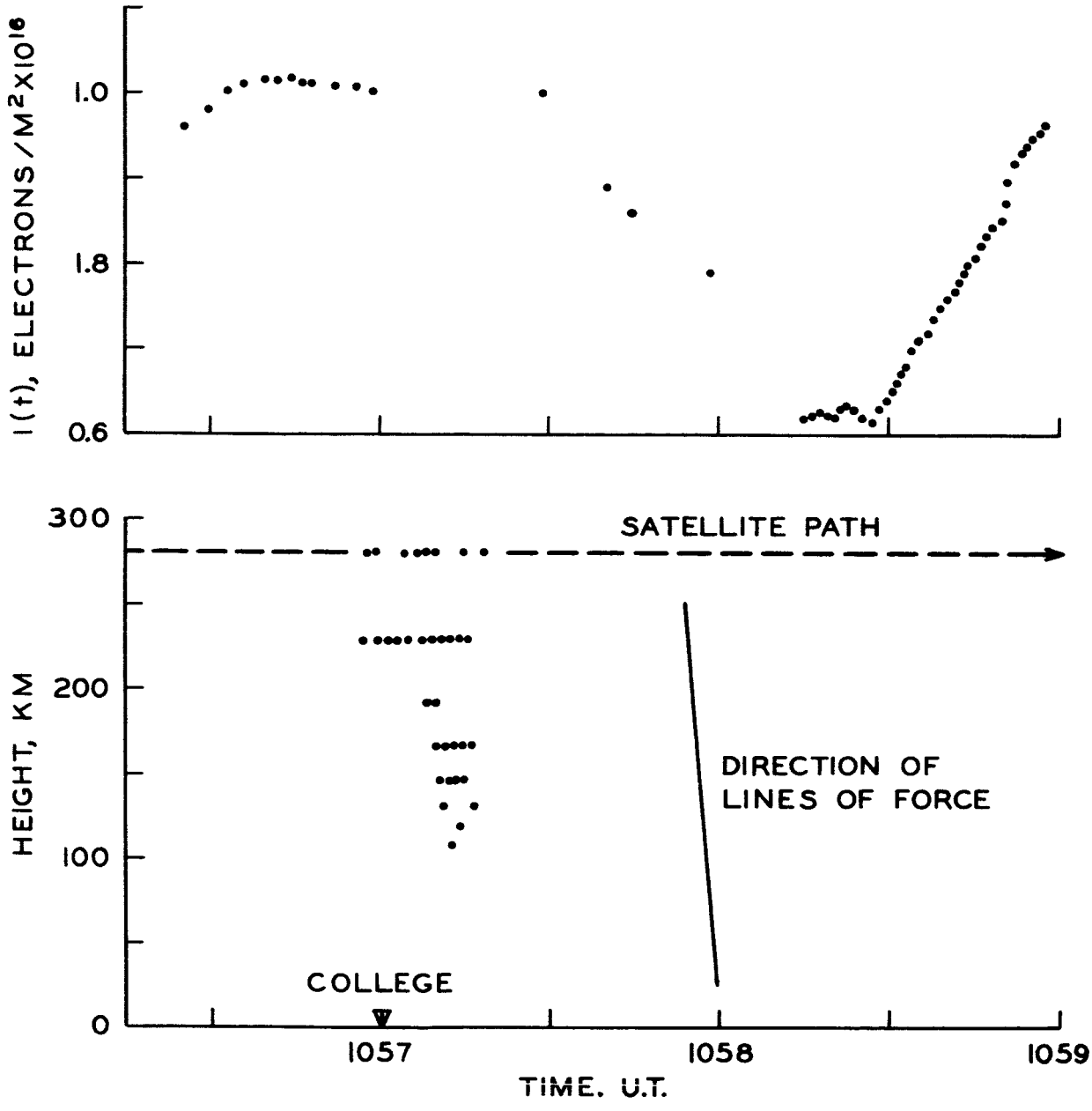

Fig. 7. The electron content as a function of time (top) and the distribution of irregularities in the plane of the magnetic meridian (bottom) for passage number 3.

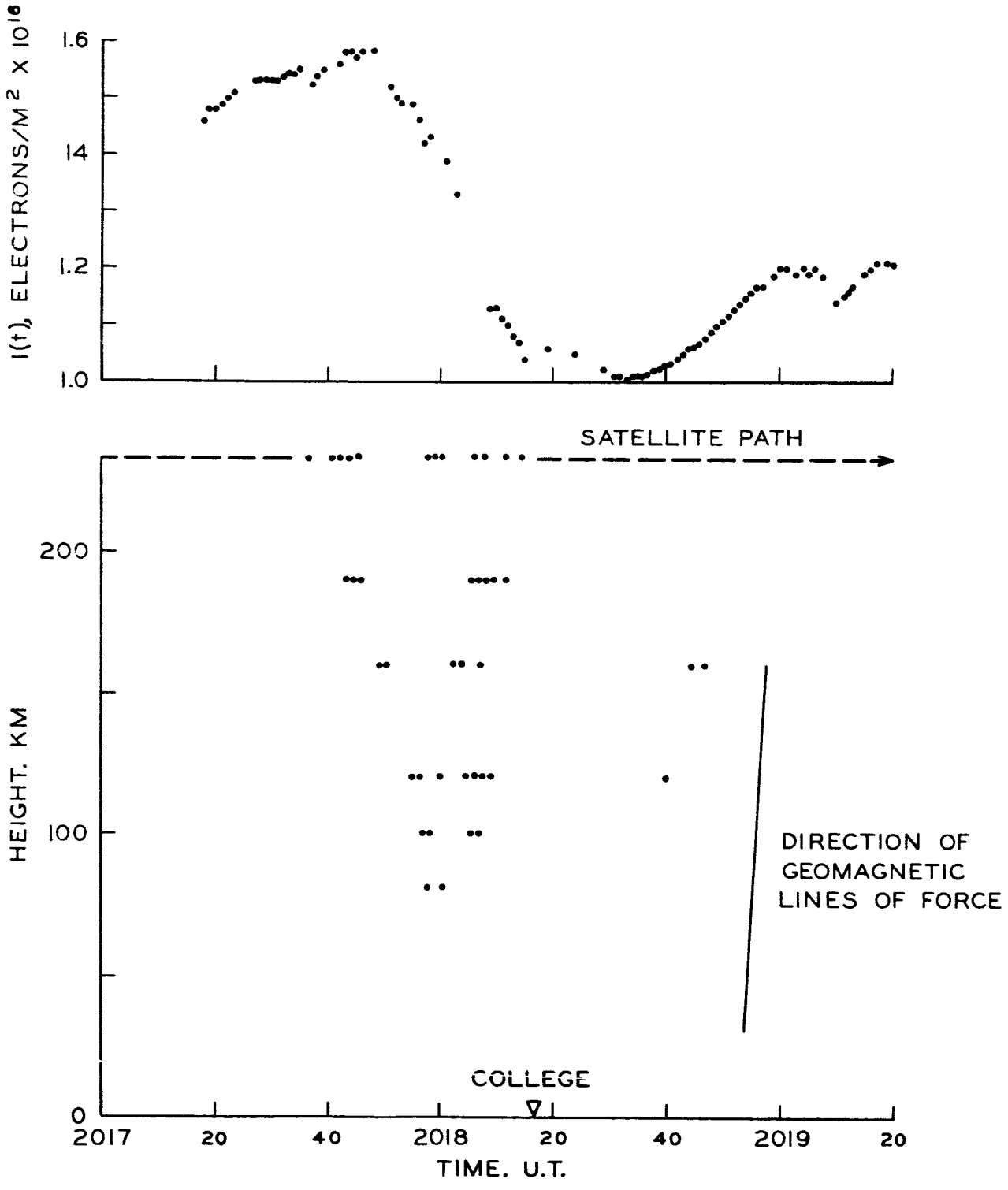

Fig. 8. The electron content as a function of time (top) and the distribution of irregularities in the plane of the magnetic meridian (bottom) for passage number 4.

2018:10 UT. Since the irregularities are north of College, the path of propagation passes through most of the diffracting irregularities when the satellite was just to the north of the region of irregularities. Just to the south of College a rather small region of irregularities was found. Corresponding to this smaller region of irregularities, a smaller increase in the electron content was observed.

CHAPTER VII

DISCUSSION OF THE RESULTS

In calculating the electron content it has been assumed that time variations in electron density can be neglected over the period in which the data was taken. The data in this case was recorded for a period ranging from one to three minutes. For the undisturbed auroral ionosphere, one would not expect significant changes in ionization to occur in a three minute period. We shall assume that an undisturbed ionosphere exists in the region where the data was taken when the local magnetic, local $K_p < 3$, earth current and cosmic noise records were undisturbed. Time variations in the intensity and motion of visual aurora would also serve to indicate the time dependence of ionization.

During the four passages of the satellite, magnetic, earth current, and absorption records were relatively quiet. For those passages in which optical auroral measurements are available, the intensity and motion of the aurora did not vary significantly. The slight southward motion of the aurora was observed during satellite passage number 1. In a two minute period between 1039 and 1041 UT the approximate motion of the observed auroral form is indicated in Figure 9. For the data used in this analysis we have assumed that time variations in ionization could be neglected in the calculation of the electron content. During a magnetic storm the electron content in the

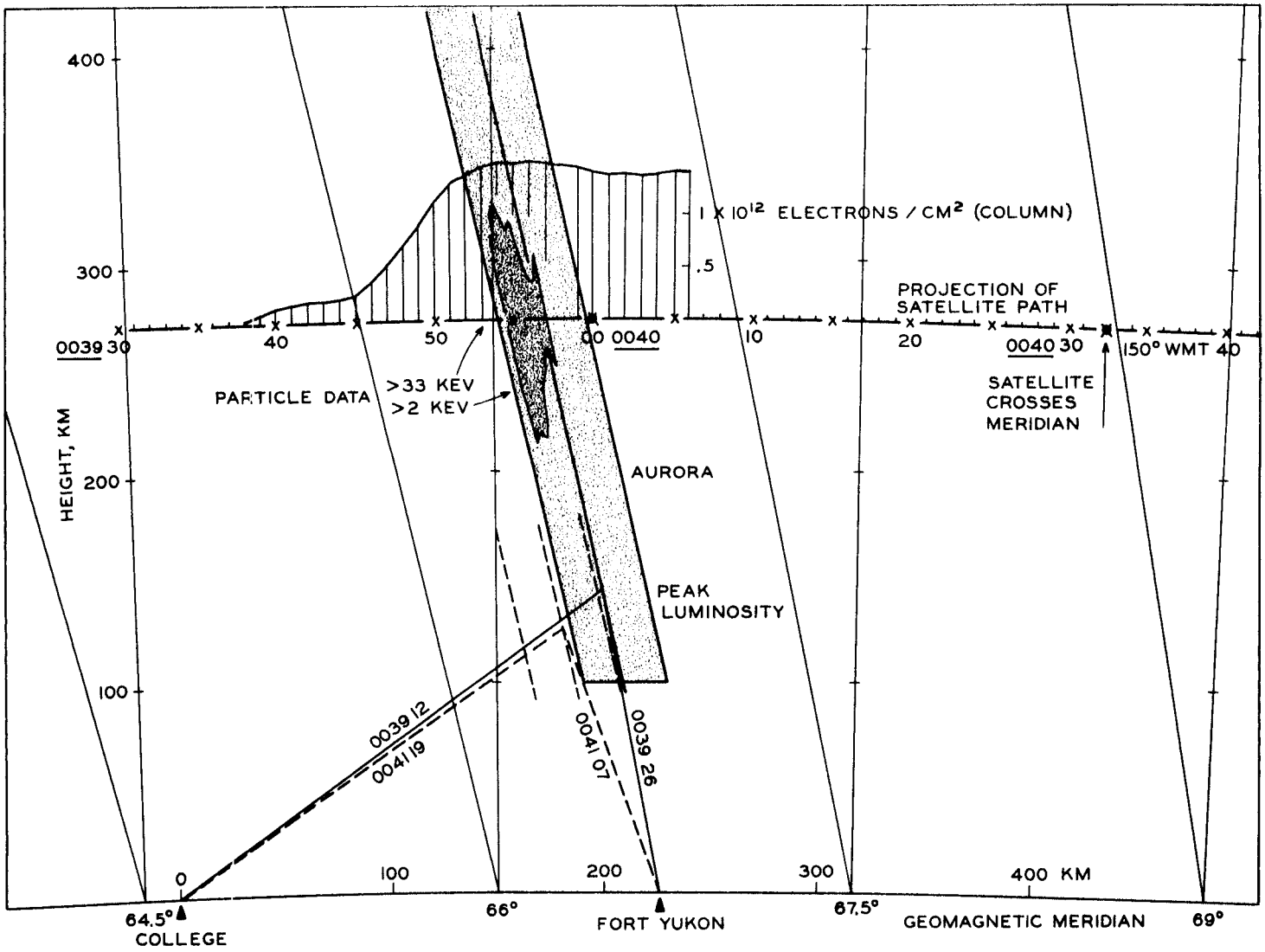

Fig. 9. The electron content after subtracting its normal value is plotted in the plane of the magnetic meridian. Also shown is the distribution of auroral luminosity and the time when energetic particle fluxes were detected.

auroral zone due to particle bombardment may change considerably in a period of one minute. The electron content obtained from differential Doppler or Faraday rotation data would under these conditions contain an undetermined component due to the time rate of change in the electron density along the path of propagation.

Passage number 1 of the satellite is of particular interest since good morphological agreement was obtained between the region of auroral luminosity and the incident particle flux. As one would expect, an increase in the electron content occurs in the region where the primary particle flux was observed. A more graphic illustration, than shown in Figure 5, of the relationship between the increase in electron content and the incident particle flux is shown in Figure 9. Shown in the plot of the electron content in Figure 9 is the difference between the normal and total oblique electron content. This normal value was obtained by taking the average value of I observed before 1039:43 UT (Figure 5). The total oblique electron content is the calculated electron content along the phase path from the satellite to the receiving antenna and in this case the obliguity of the phase path is not accounted for by converting the calculated electron content to an equivalent vertical column.

The excess electron content shown in Figure 9 is probably due to ionization by the primary particle flux. The plot suggests that the region of increased electron density extends

somewhat south of the auroral form. Why this region of high ionization south of the auroral form should exist cannot be accounted for by the particle flux measured unless the recombination rate of electrons with molecular ions is sufficiently slow to allow diffusion of the electrons. Estimates of electron recombination rates up to approximately 200 km are much too rapid and estimates of recombination rates above 200 km are uncertain (Chamberlain, 1961). Another explanation for increase in the electron content south of the auroral form is that it may be due to low energy protons which could not be measured by the total energy detectors. The photometer data from College and Fort Yukon show a wide-spread hydrogen emission, beyond the limits of the discrete auroral form and, therefore, it is possible that protons were incident over a larger region than the observed particle flux.

A plot similar to Figure 9 for passage number 2 is shown in Figure 10. The increase in the electron content corresponds well with the measured particle flux to at least 1049 UT. Since the particle data acquisition ended 1048:38 UT, it is not known whether or not the increase in electron content observed after 1049:00 UT is also possibly associated with incident particles.

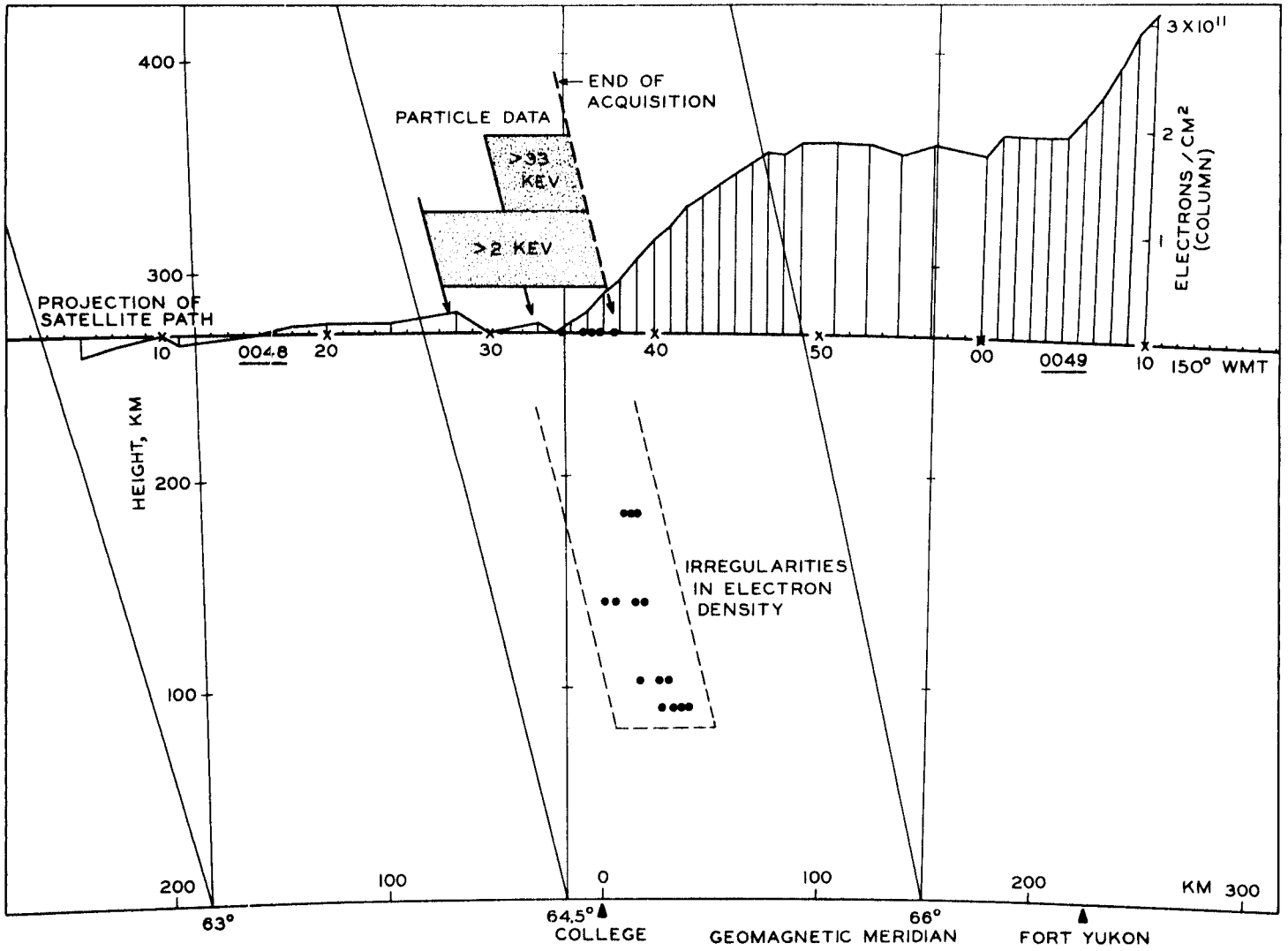

Fig. 10. The electron content after subtracting its normal value is plotted in the plane at the magnetic meridian. Also shown is the distribution of diffracting irregularities in electron density and the time when energetic particles were detected.

CHAPTER VIII

CONCLUSIONS

The results of the experiment indicata a good morphological correlation between electron content variations, regions of auroral luminosity, and incident particle fluxes. Large horizontal gradients were found to exist during all of the passages of the satellite in which differential Doppler data were obtained. Since particle data were obtained intermittently on only part of the passages, it is not known whether or not ionization by primary particles is the only mechanism responsible for the horizontal gradients.

As one would expect, the electron content was found to increase when the ray path of the radio wave passes through the region of auroral luminosity. The electron content, however, did not increase rapidly when the ray path penetrated the boundary of the discrete auroral form, but instead the electron density apparently increases relatively slowly as the ray path approaches the boundary of the auroral luminosity. This slow increase in the electron density is probably due to either diffusion of electrons away from the region of auroral luminosity or to a low energy proton flux having greater north-south range of incidence than the discrete auroral form. The conclusions drawn from this analysis are based on data from only four satellite passages and, therefore, they are of a tentative nature.

The determination of the electron content from the differential Doppler measurement of satellite radio transmissions is relatively new and further development of the technique will probably be made. As it has been shown, the differential Doppler measurement is quite sensitive to variations in electron density along the path of propagation and, therefore, the method has considerable value in the study of the auroral ionosphere. Furthermore, the analysis points out the value of conducting coordinated experiments in which radio, optical, and direct particle measurements are made simultaneously.

APPENDIX I

THE DETERMINATION OF THE HEIGHT OF DIFFRACTING IRREGULARITIES

A brief discussion of the method used to determine the height of diffracting irregularities in electron density is given here. The preliminary results of a recent study of satellite signal scintillation observed at College has shown that E-region diffraction does occur frequently (Hook and Owren, 1962). The subsatellite heights of the irregularities have been found rather frequently to be as low as 90 km. Furthermore, it appears that the diffracting irregularities are often distributed more or less vertically and probably parallel to the lines of force of the geomagnetic field. The north-south width of the diffracting regions at times appears to be less than 100 km.

To determine the height of irregularities in electron density, a system of three spaced receiving antennas was employed. When two of the antennas are spaced along the sub-satellite path, the ground velocity of the amplitude pattern can be obtained from time shifts between corresponding scintillations and known distance between antennas. It is necessary that the spacing between antennas be less than the average size of the individual irregularities. An antenna spacing of 170 meters was chosen after some experimentation and this spacing was found to be approximately the minimum spacing which would produce measurable time displacements between the two diffraction patterns. The height of irregularities, when

they are confined to a thin layer, is then obtained using the relation

$$h = h_s v/(v+v_s),$$

where h_s and v_s are the height and velocity of the satellite respectively and v is the measured ground velocity of the diffraction pattern. If the irregularities are not confined to a thin layer, then the velocity of the resulting diffraction pattern will be a combination of a series of diffraction patterns, all of which will have a different velocity. The observed velocity of the diffraction pattern for such a thick region of irregularities will be a certain weighted mean velocity.

It has been found rather frequently that the calculated height of irregularities will systematically increase or decrease in height as a function of time. Upon projecting the calculated position in space of the irregularities of the College geomagnetic meridian, it appears that the irregularities are distributed more or less vertically and possibly parallel to lines of force of the geomagnetic field. It has been assumed that refraction along the path of propagation is small, so the radio wave propagates essentially along a straight line.

APPENDIX II

FORTRAN COMPUTER PROGRAMS

The Fortran computer programs given here are specifically programed for the University of Alaska's IBM 1620 Computer.

The Fortran program given below is used to calculate the distance from the satellite to the ground station and the cosine of the zenith angle. The input data requires the geographic latitude, longitude, and height of the satellite at given intervals of time.

```
      READ 1,LT2,LNG2
      READ 3,N
      PRINT 5
      D=SIN(LT2*0.01745)
      E=COS(LT2*0.01745)
      F=LNG2*0.01745
      DO 2 I=1,N
      READ 7 X,Y,Z
      A=X*0.01745
      B=Y*0.01745
      R1=R2+Z
      RD=SQRT(R1*R1+R2-2.*R1*R2*(COS(A)*D*COS(B-F)+SIN(A)*E)
      C=(RD*RD+R2S-R1*R1)/(2.0*RD*R2)
    2 PRINT 9,RD,C
    1 FORMAT(F6.2,F6.2)
    3 FORMAT(I4)
    7 FORMAT(F8.2,F8.2,F8.2)
    9 FORMAT(F8.2,17X,F8.5)
    5 FORMAT(15H RADIAL DIST(KM),10X,17HCOS(ZENITH ANGLE)
      END
```

The following Fortran program is used to find the value of ΔP_o by minimizing the value of S. The minimization is done by trying values of ΔP_o until the minimum is established. Graphical

techniques can be used to choose values of ΔP_o so that the trial and error process will converge more rapidly.

```
      DIMENSION DP(200),X(200),Y(200),DPI(200)
      READ 1,B
      READ 2,XO
      READ 3,N
      READ 10,DPC
      DO 4 I=1,N
    4 READ 5,DP(I)
      DO 6 J=1,N
    6 READ 7,X(J)
      DO 8 K=1,N
    8 READ 9,Y(K)
      DO 40 M=1,N
   40 READ 41,DPI(M)
   14 PAUSE
      S=0.
      READ 20,DPO
      DO 12,L=1,N
      A=B*(XO*DPC+(DPO+DPI(L))*Y(L))/X(L)
   12 S=S+(A-DP(L))*(A-DP(L))
      PRINT 30,DPO,S
      GO TO 14
      1FORMAT(F4.2)
      2FORMAT(F6.5)
      3FORMAT(14)
      5FORMAT(F3.1)
      7FORMAT(F6.5)
      9FORMAT(F6.5)
      10FORMAT(F6.1)
      20FORMAT(F6.1)
      30FORMAT(F6.1,10X,F14.5)
      41FORMAT(F6.1)
      END
```

The program below is used to find a third degree polynomial to fit a set of up to 20 data points. The least square method is used to find the polynomial.

```
      DINEMSION X(20),Y(20)
      READ 16,N
      DO 9I=1,N
    9 READ 10,X(I),Y(I)
```

```
      S1=0.
      S2=0.
      S3=0.
      S4=0.
      S5=0.
      S6=0.
      S7=0.
      S8=0.
      S9=0.
      S10=0.
      DO 3 I=1,N
      S1=S1+X(I)
      S2=S2+X(I)*X(I)
      S3=S3+X(I)*X(I)*X(I)
      S4=S4+X(I)**4.
      S5=S5+X(I)**5.
      S6=S6+X(I)**6.
      S7=S7+Y(I)
      S8=S8+X(I)*Y(I)
      S9=S9+X(I)*X(I)*Y(I)
    3 S10=S10+X(I)*X(I)*X(I)*Y(I)
      F1=S4*S6-S5*S5
      F2=S3*S5-S4*S4
      F3=S2*S6-S3*S5
      F4=S2*S5-S3*S4
      F5=S2*S4-S3*S3
      F6=S3*S6-S4*S5
      F7=S9*S6-S5*S10
      F8=S9*S5-S10*S4
      F9=S9*S4-S10*S3
      F10=S2*S10-S3*S9
      F11=S3*S10-S4*S9
      F12=S4*S10-S5*S9
      XN=N
      P1=XN*(S2*F1-S3*F6+S4*F2)-S1*(S1*F1-S3*F3+S4*F4)
      P2=S2*(S1*F6-S2*F3+S4*F5)-S3*(S1*F2-S2*F4+S3*F5)
      DNOM=P1+P2
      P3=S7*(S2*F1-S3*F6+S4*F2)-S1*(S8*F1-S3*F7+S4*F8)
      P4=S2*(S8*F6-S2*F7+S4*F9)-S3*(S8*F2-S2*F8+S3*F9)
      A=(P3+P4)/DNOM
      P5=XN*(S8*F1-S3*F7+S4*F8)-S7*(S1*F1-S3*F3+S4*F4)
      P6=S2*(S1*F7-S8*F3+S4*F10)-S3*(S1*F8-S8*F4+S3*F10)
      B=(P5+P6)/DNOM
      P7=XN*(S2*F7-S8*F6+S4*F11)-S1*(S1*F7-S8*F3+S4*F10)
      P8=S7*(S1*F6-S2*F3+S4*F5)-S3*(S1*F11-S2*F10+S8*F5)
      C=(P7+P8)/DNOM
      P9=XN*(S2*F12-S3*F11+S8*F2)-S1*(S1*F12-S3*F10+S8*F4)
      P10=S2*(S1*F11-S2*F10+S8*F5)-S7*(S1*F2-S2*F4+S3*F5)
      D=(P9+P10)/DNOM
      PRINT 11,A,B,C,D
      IF(SENSE SWITCH1) 30,40
   30 READ 18,NN,L
      DO 6 11=5,NN,L
```

```
      J=11-5
      XJ=J
      IF (SENSE SWITCH 2) 50,60
   60 XXJ=XJ*.01
      E=A+B*XXJ+C*XXJ*XXJ+D*XXJ**3.
      GO TO 6
   50 E=A+B*XJ+C*XJ*XJ+D*XJ**3.
    6 PRINT 12,J,E
      PAUSE
   40 READ 4,T
      IF (T) 21,22,21
   21 IF (SENSE SWITCH 2) 70,80
   70 F=A+B*T+C*T*T+D*T**3.
      GO TO 85
   80 TT=T*.01
      F=A+B*TT+C*TT*TT+D*TT**3.
   85 PRINT 23,T,F
      GO TO 40
   22 PAUSE
      16FORMAT(I3)
      10FORMAT(F10.5,F10.5)
      11FORMAT(2HA=F10.5,/2HB=F10.5,/2HC=F10.5,/2HD=F10.5)
      12FORMAT(I4,8X,F10.5)
      18FORMAT(I4,I4)
      4FORMAT(F7.2)
      23FORMAT(F7.2,8X,F10.5)
      END
```

The following program is used to calculate the time derivative of the zenith angle. This program requires that the zenith angle as a function of time be represented by a third degree polynomial.

```
      DIMENSION T(60)
   20 READ 8,N
      IF(N-1) 12,12,10
   10 READ 2,A,B,C,D
      DO 3 I=1,N
      READ 4,T(I)
      Z=A*T(I)**3.+B*T(I)*T(I)+C*T(I)+D
      E=(3.*A*T(I)*T(I)+2.*B*T(I)+C)*.01
      TT=T(I)*100.
      IF (SENSE SWITCH 1) 30,40
   30 PRINT 6,TT,Z,E
      GO TO 3
   40 PUNCH 16,Z
```

```
      PUNCH 14,E
    3 CONTINUE
      GO TO 20
   12 PAUSE
      2FORMAT  (F8.5,F8.5,F8.5,F8.5)
      4FORMAT  (F7.4)
      6FORMAT  (F7.2,8X,F8.5,8X,F8.5)
      16FORMAT (F8.5)
      8FORMAT  (I3)
      14FORMAT (F8.5)
      END
```

The following program is used to calculate the electron content of a column having a base of unit area (electrons/m^2 column). The input data required consists of tabulated values of $\cos X_i$ and $\Delta \dot{P}_i$ and the initial condition ΔP_o.

```
      DIMENSION X(200),DP(200)
      READ 1,N
      READ 3,F
      READ 5,G
      READ 7,DPO
      PRINT 20
      DO 8 I=1,N
    8 READ 9,X(I)
      DO 1D J=1,N
   10 READ 11,DP(J)
      DO 12 K=1,N
      A=(F**2.0)*G*X(K)*(DPO+DP(K))/40.3
      BN=K
   12 PRINT 21,BN,A
    1 FORMAT(I4)
    3 FORMAT(E10.1)
    5 FORMAT(F4.1)
    7 FORMAT(F6.1)
    9 FORMAT(F6.5)
   11 FORMAT(F3.1)
   20 FORMAT(5X,2HNO,6X,16H COLUMNAR DENSITY)
   21 FORMAT(3X,F4.0,10X,E9.3)
      END
```

Hibberd, F.H., and J.A. Thomas, The Determination of Electron Distribution in the Upper Ionosphere from Satellite Doppler Observations, J. Atmosph. Terr. Phys., 17 1/2, 71-81, 1959.

Hook, J.L., and Leif Owren, The Vertical Distribution of E-Region Irregularities Deduced from Scintillations of Satellite Radio Signals, J. Geophys. Research, 67, 5353, 1962.

Little, C.G., and R.S. Lawrence, The Use of Polarization Fading of Satellite Signals to Study the Electron Content and Irregularities in the Ionosphere, J. Research NBS, 64D, 4, 1960.

Nisbet, J.S., and S.A. Bowhill, Electron Densities in the F-Region of the Ionosphere from Rocket Measurement, 1 and 2, J. Geophys. Research, 65(11), 3601-3614, 1960.

Meyerott, R.E. and J.E. Evans, A Program of Coordinated Particle, Optical, and Radio Measurements on Auroras. Paper presented at the Western National Meeting of the American Geophysical Union held at Stanford University, California, 1962.

Ratcliffe, J.A., The Magneto-Ionic Theory and Its Applications to the Ionosphere, Cambridge University Press, 1959.

Rawer, Karl, The Ionosphere, Frederick Ungar Publishing Co., New York, 1952.

Ross, W.J., The Determination of Ionosphoric Electron Content from Satellite Doppler Measurements, 1 and 2, J. Geophys. Research, 65(9), 2601-2615, 1960.

Seddon, J.C., Propagation Measurements in the Ionosphere with the Aid of Rockets, J. Geophys. Research, 58(3), 323, 1953.

Weekes, K., On the Interpretation of the Doppler Effect from Senders in an Artificial Satellite. J. Atmosph. Terr. Phys. 12, 335, 1958.

Yeh, K.C., and G.W. Swenson, Jr., Ionospheric Electron Content and Its Variations Deduced from Satellite Observations, J. Geophys. Research, 66, 1061-1067, 1961.